

Synthesis of MoS₂ nanorods and their catalytic test in the HDS of dibenzothiophene

M A Albiter, R Huirache-Acuña, F Paraguay-Delgado,

J L Rico and G Alonso- Nuñez

Abstract

Partially sulfided nanostructures were synthesized by direct sulfurization of α -MoO₃ nanorods using a mixture of H₂S/H₂, 15 vol%, at several temperatures (400, 500, 600, 700, and 800 °C). These materials were tested as catalysts in the hydrodesulfurization (HDS) of dibenzothiophene (DBT) and characterized by specific surface areas using the expression developed by Brunauer, Emmett, and Teller (BET equation), x-ray diffraction (XRD), scanning electron microscopy (SEM) and transmission electron microscopy (TEM). The TEM images show a gradual evolution from a smooth surface to a rough material, presenting some type of holes all over the particles, but keeping their rod-like structure throughout sulfidation. The results of evaluating the catalysts in the HDS of DBT showed that the best temperature for sulfidation is 500 °C. In all samples, a higher selectivity for hydrogenation over sulfur removal was observed.

1. Introduction

Since the discovery of carbon nanotubes in 1991 [1], layered metal dichalcogenides such as MoS₂ have also been obtained as nanostructures; the first synthesis was reported in 1992 [2]. Transition metal dichalcogenides have a wide range of interesting physical properties such as lubricants [3]. With the synthesis and characterization of MoS₂ and WS₂ nanostructures, a wide field of research has

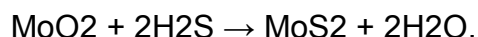
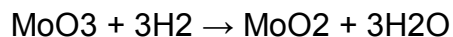
been opened up and permitted to achieve the synthesis of other metal dichalcogenide structures [4]. Subsequently, many other preparation methods for MoS₂ nanostructures have been explored to produce nanotubes, for example: using iodine vapour transport of MoS₂ powder in a vacuum at 740 °C [5]; thermal decomposition of ammonium thiomolybdate at 450 °C [6]; simple heating of MoS₃ in hydrogen steam at high temperature (1300 °C) [7]; heating MoS₂ powder covered by Mo foil at 1300 °C in the presence of H₂S [8]; electrodepositing nanowires size-selectively on a highly oriented pyrolytic graphite (HOPG) surface, then conversion to MoS₂ by exposure to H₂S at 800–900 °C [9]; using a template method to synthesize twisted MoS₂ nanotubes [10]; soaking MoS₂ micrometre-sized particles in an acid solution and then sonicating in ethanol to obtain lamellar MoS₂, a further sonication leading to nanorod formation [11]; and finally, synthesizing nanotubes and nanorods of MoS₂ by utilizing a hydrothermal method at low temperature (180 °C) with MoO₃ and potassium thiocyanate as reactants [12]. Our study presents the synthesis of nanostructures of MoS₂ at different sulfidation temperatures (400, 500, 600, 700, 800 °C), preserving the precursor morphology (one dimensional nanostructures of α -MoO₃) during the activation process. By making smaller particle sizes, increases in the specific surface area and the number of active sites are expected. As an example, a correlation between HDS activity and one-dimensional (1D) structures in commercial catalysts was reported recently [13]. The HDS of DBT was performed to study the hydrotreating properties of this sulfide structure. HDS is a key process in oil refining for lowering the sulfur content in fuels. Lately, environmental laws in this matter have been enforced, leading to the research and

development of new catalysts suitable for more efficient sulfur removal. DBT is an appropriate model compound to use in our experiments due to its difficulty for HDS. It is known that the reactivity of sulfur compounds follows the order: thiophene > benzothiophene > dibenzothiophene.

2. Experimental details

2.1. Catalysts preparation

The α -MoO₃ nanorods were synthesized using the hydrothermal method reported elsewhere [14], with some modifications. Instead of ageing the saturated solution of ammonium heptamolybdate tetrahydrated (AHM, (NH₄)₆Mo₇O₂₄·4H₂O) for a month or more as reported in the above reference, it was stirred at 60 °C for a week. A typical synthesis comprised 5 ml of the prepared AHM solution diluted with 5 ml of deionized water and then acidified with a 2.2 N nitric acid solution (5 ml). The resulting solution was transferred to a Teflon-lined stainlesssteel autoclave and heated at 200 °C for 30–60 h. The resultant materials were washed using deionized water and dried for 5 h at 60 °C. Finally, they were sulfided under a mixture of H₂S/H₂ (15 vol% of H₂S) for 4 h at several temperatures (400, 500, 600, 700 and 800 °C). The obtained catalysts were labelled MS-400, MS-500, MS-600, MS-700 and MS-800, according to the sulfidation temperature. The thermal transformation from α -MoO₃ to MoS₂ can be represented as follows:



The first reduction takes place at temperatures as low as 50 °C and continues until 350 °C [15], and a further sulfidation yields MoS₂.

2.2. Catalytic activity and selectivity

The HDS of DBT was carried out in a Parr Model 4520 highpressure batch reactor with a volume of one litre equipped with a magnetically driven turbine, which allows homogenous dispersion of the gas into the liquid phase. One gram of catalyst was placed in the reactor together with the reactant mixture (5 vol% of DBT in decaline; total volume 150 ml). The reactor vessel was first purged and then pressurized with hydrogen to 3.3 MPa, and heated to 350 °C at 10 °C min⁻¹ with a stirring speed of 600 rpm. Once at 350 °C, this reaction was followed for 5 h, analysing samples of the reactant mixture every 30 min using a Perkin-Elmer Clarus 500 gas chromatograph with an attached autosampler and equipped with a 9 foot long packed column containing 3% OV-17, on Chromosorb WAW 80/100 as a separating phase. After catalytic evaluation, the samples were separated from the reaction mixture by filtration, then washed with 2-propanol to remove residual reaction products and dried at room temperature to further characterization. The HDS of DBT yields biphenyl (BP) through the so-called direct desulfurization pathway (DDS) and cyclohexilbenzene (CHB) and tetra hydrodibenzothiophene

Table 1. Shows S/Mo atomic ratios obtained by EDS before and after HDS of DBT.

Catalyst	S/Mo ratio	
	Before HDS	After HDS
MS-400	0.07	0.10
MS-500	0.92	1.54
MS-600	1.11	1.51
MS-700	1.64	1.79
MS-800	1.80	1.78

(THDBT) through the hydrogenative pathway (HYD). Since these two

pathways are parallel and competitive, the selectivity (HYD/DDS) is determined by [16]:

$$\text{HYD/DDS} = ([\text{CHB}] + [\text{THDBT}]) / [\text{BP}].$$

2.3. Material characterization

All materials were characterized before and after the catalytic test. Specific surfaces areas were measured using a Quantachrome Nova 1000 series by nitrogen adsorption at $-196\text{ }^{\circ}\text{C}$, using the BET method. Samples were degassed under vacuum at $250\text{ }^{\circ}\text{C}$ before nitrogen adsorption. X-ray diffraction (XRD) studies were performed using a Philips XPert MPD Diffractometer, equipped with a curved graphite diffracted beam monochromator, using Cu $K\alpha$ radiation ($\lambda = 1.54184\text{ \AA}$) and operated at 43 kV and 30 mA. Catalyst morphology and elemental analysis were studied using a JEOL JSM-5800 LV scanning electron microscope, analysing several fields at different magnifications. The elemental composition was determined using energy-dispersive x-ray spectroscopy (EDS). Relative atomic ratios were calculated for all samples before and after HDS evaluation. A Philips CM200 analytical transmission electron microscope operated at 200 kV with a LaB6 filament was used to study the materials. Using a Gatan Parallel Electron Energy Loss Spectrometer (PEELS model 766), spectra were taken in diffraction mode with 0.1 eV/ch dispersion, an aperture of 3 mm and a collection semi-angle of 4.9 mrad.

3. Results and discussion

3.1. Elemental analysis

The S/Mo ratios, obtained by EDS, are reported in table 1. A higher S/Mo ratio was detected when the sulfurization temperature increased. Accordingly, the

materials are not completely sulfided, since the S/Mo atomic ratios are below the theoretical value of two. It is proposed that sulfidation progresses from the outer to the inner portion of the particles (figure 1). Nanoribbons have a low mass/surface ratio and are easily sulfided, in contrast to nanorods, which show a higher mass/surface ratio. This behaviour was also observed for the synthesis of onion-like nanostructures, which present, at the end, an oxide core surrounded by MoS₂ layers [2]. According to table 1, a variation in the S/Mo ratio from 0.07 to 1.8 indicates the gradual sulfurization of α -MoO₃ as the temperature increases from 400 to 800 °C. Moreover, the rodlike morphology remains for all materials when activated under H₂S/H₂, in contrast to other similar activation techniques [22].

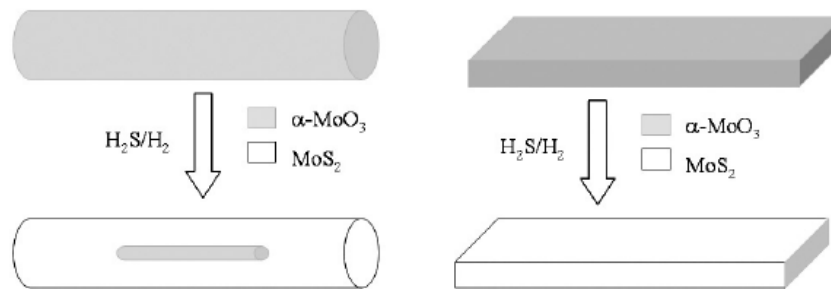


Figure 1. Sulfidation process in nanostructures.

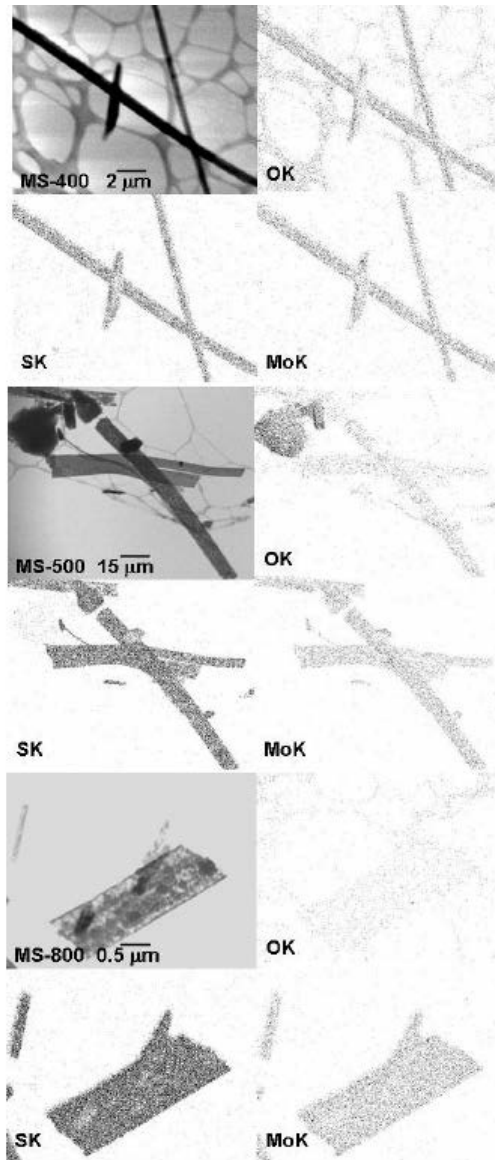


Figure 2. STEM elemental mapping by EDS for samples MS-400, MS-500 and MS-800.

An increase in the S/Mo atomic ratio throughout HDS was observed, except for the MS-800 sample, for which values remain almost the same before and after HDS. This increase is due to further reduction and sulfidation throughout HDS of DBT. Figure 2 shows scanning transmission electron microscopy (STEM) elemental mapping images of oxygen (O),

Table 2. Specific surface areas before and after HDS of DBT.

Catalyst	Specific surface areas (± 0.5) $\text{m}^2 \text{g}^{-1}$	
	Before HDS	After HDS
$\alpha\text{-MoO}_3$	11.7	—
MS-400	11.6	5.1
MS-500	13.9	10.2
MS-600	19.9	20.8
MS-700	13.8	3.6
MS-800	3.6	0.5

sulfur (S) and molybdenum (Mo) for samples MS-400, MS- 500 and MS-800. Here it is evident how the gradual sulfidation process occurs, showing a decrease in O content and an increase in S as the activation temperature increases. In the case of MS-800, it is evident that oxygen is practically gone compared with MS-400 or MS-500. Another technique used to study the sulfidation progress in the nanostructures as a function of temperature was electron energy loss spectroscopy (EELS) analysis. Figure 3(a), shows the characteristic edges generated by the precursor (MO), MS-400, MS-500, MS-600 and MS-800. In figure 3(b), the oxygen edge is zoomed in to observe the change in intensity when the sulfidation temperature increases. Simultaneously to the disappearance of the signal for oxygen, the sulfur edge (figure 3(c)) starts to grow. It can be observed that, at sulfidation temperatures higher than 500 °C, the oxygen signal disappears and that sulfur grows (figures 3(b), (c)).

3.2. Specific surface area

The specific surface areas of samples before and after HDS are listed in table 2. The largest value was observed for catalysts obtained at 600 °C and the lowest was observed for MS-800 (around 20 and 4 $\text{m}^2 \text{g}^{-1}$, respectively). All specific

surface areas diminish after HDS except for catalyst MS-600, the value of which remained practically the same. Usually, the reduction in the specific surface area is attributed to carbon deposition during HDS, blocking the catalyst surface. A direct correlation between the surface area and the catalytic activity was not observed in the present study. However, their activities are comparable to those reported for molybdenum sulfide catalysts synthesized from thioalkylmetallates, following ex situ activation [20].

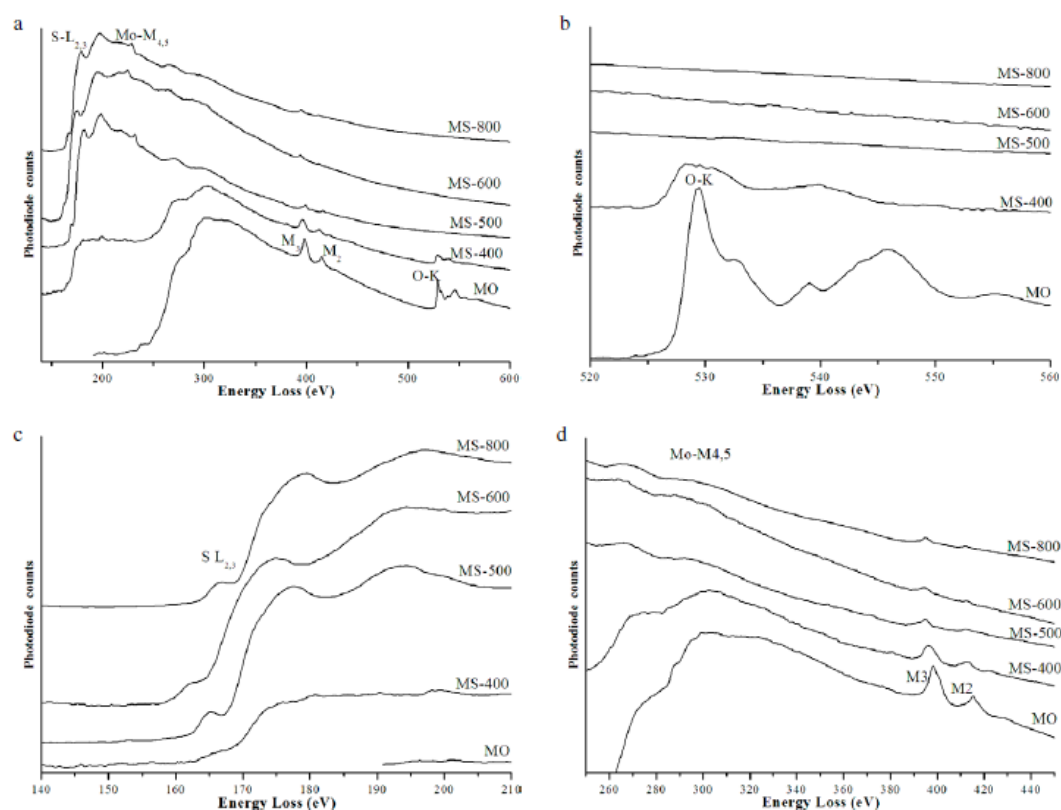


Figure 3. Electron energy loss spectroscopy of materials: (a) general, (b) oxygen, (c) molybdenum and (d) sulfur.

3.3. X-ray diffraction

Collected XRD patterns for catalysts before HDS are shown in figure 4(a), and those for spent samples are shown in figure 4(b). In figure 4(a), the peaks (020)

and (060) for the precursor, α -MoO₃ (MO, JCPDS card 75-912), disappear after being treated with H₂S at temperatures of 400 or 500 °C; two new structures MoO₂ and MoS₂ are generated and were identified by using the 32-671 and 37-1492 JCPDS cards, respectively. This means that MS-400 and MS-500 did not reach a complete sulfided state when activated at 400 or 500 °C. In contrast, the catalysts MS-600, MS-700 and MS-800 do not show the presence of the MoO₂ phase (figure 4(a)). XRD is a suitable technique for giving information on the sulfuration process. The (002) peak for MoS₂ increases intensity at 500 °C and keeps growing at higher activation temperatures. At 800 °C, it reaches an almost completely sulfiding state with a S/Mo ratio of 1.8; this value is similar to those reported for other MoS₂-based catalysts [24]. The XRD patterns of the spent catalysts exhibit insignificant changes after HDS (figure 4(b)) except MS-500, which presents a more intense (002) peak at $2\theta = 14^\circ$ but still shows a certain amount of MoO₂ phase ($2\theta = 26^\circ, 38^\circ, 53^\circ$); however, the (111) had a drastic reduction. The $\bar{1}$ peak transitions were attributed to the H₂S formation in the reactor during HDS of DBT [17], giving the conditions for further sulfidation. Two interesting remarks should be mentioned. First, the (111) and ($\bar{1}$ 312) planes seem to appear for MS-600 after the $\bar{1}$ HDS catalyst, which could be explained by assuming that reaction conditions somehow permitted the partially sulfided particles to expose their oxide cores. The second situation is that, when MO (α -MoO₃) was activated in situ, it presented a similar pattern to that of MS-500. The latter behaviour will be addressed in more detail in an ongoing work [18].

3.4. Scanning electron microscopy

Figures 5 and 6 show SEM micrographs of catalysts before (figures 5(a)–(c),

6(g)–(i) and after (figures 5(d) and (e), 6(j)– (l)) HDS of DBT. The average diameter of the rods is around 300 nm, in a range from 100 to 700 nm. It is interesting to observe that, after sulfidation at 400 °C, the MS-400 (figures 5(b) and (e)) still exhibits some irregular particles, as α -MoO₃ (figures 5(a) and (d)) shows. MS-500 (figures 5(c) and (f)), MS-600 (figures 6(g) and (j)), MS-700 (figures 6(h) and (k)) and MS-800 (figures 6(i) and (l)) samples show similar structures before and after the catalytic test, however some small particles formed throughout HDS. These images show that insignificant changes occurred throughout HDS,

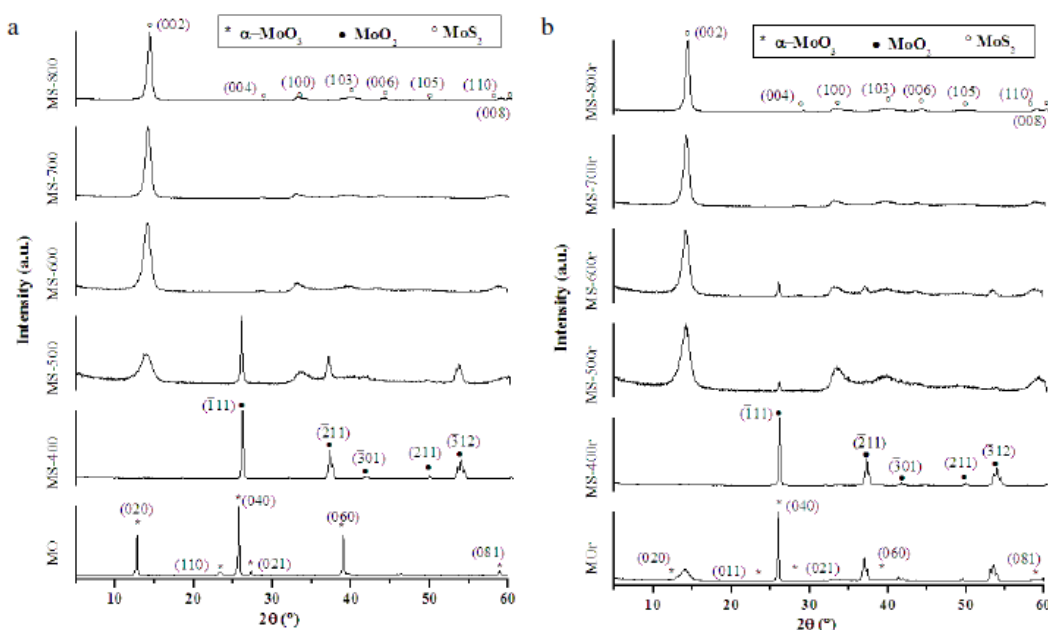


Figure 4. XRD patterns of catalytic materials before (a) and after (b) HDS of DBT.

showing indirectly, good structural resistance. In some cases, the structure of a catalyst subjected to the HDS experimental conditions collapses or become agglomerated, as mentioned recently [19].

3.5. Transmission electron microscopy

Figure 7 shows TEM micrographs taken to monitor the sulfurization progress

from α -MoO₃ to MoS₂ at several temperatures. All samples preserved the rod-like precursor morphology, but crystalline changes occurred from orthorhombic to hexagonal, exposing some holes along the rods, which were not observed in the precursor surface (figure 7(a)). This phenomenon is particularly evident in MS-700 and MS-800 samples (figures 7(e) and (f)). The formation of these holes could be explained by assuming that, during the replacement of oxygen by sulfur, some bending and rearrangement of the MoS₂ basal planes occurred [20, 21]. TEM micrographs for selected spent catalysts (MS-400, MS- 500 and MS-800) are presented in figure 8, and show insignificant changes throughout HDS. Regarding crystalline transitions involved during the synthesis of these materials, the structure changes from orthorhombic (α -MoO₃) to monoclinic (MoO₂) and finally becomes hexagonal (MoS₂). In agreement with the XRD patterns in the bulk and the selected electron diffraction (SAED) patterns in localized zones (attached to the micrographs in figures 7 and 8), most of the chosen particles were MoS₂. In table 4 the lattice spacing values are listed, where most of them belong to MoS₂ and only some of the selected particles (MS-400, MS-500 and MS-700) present

Table 3. Catalytic activity and selectivity in HDS of DBT.

Catalyst	$k(10^7)$ ($\text{mol s}^{-1} \text{g}_{\text{cat}}^{-1}$)	% DBT conversion (mol%)	Selectivity HYD/DDS
MS-400	2.80	16.60	1.92
MS-500	3.40	20.04	2.17
MS-600	2.37	12.58	1.64
MS-700	2.31	12.66	1.17
MS-800	2.84	15.10	1.25

diffracted planes for α -MoO₃. At the beginning of sulfidation, the α -MoO₃ shows a defined crystalline pattern (figure 7(a)), which transformed to a

polycrystalline concentric-ring pattern when converted to MoS₂ (figures 7(d)–(f)). The MS- 500 SAED (figure 7(c)) clearly shows the presence of the crystalline and polycrystalline structures α -MoO₃ and MoS₂, respectively. However, further studies are required in order to clarify how this crystalline transition occurs; we suggest a transformation from α -MoO₃ to MoS₂, as shown in the figure 9.

3.6. Catalytic activity and selectivity

Table 3 shows the activity and selectivity results of catalysts in the HDS of DBT. Even though MS-500 catalyst is partially sulfided, it showed the highest DBT conversion and the highest activity. Concerning selectivity, typical low HYD/DDS ratios are commonly observed in industrial CoMo/Al₂O₃ catalysts, favouring the DDS reaction pathway [13, 14]. On the other hand, our values are indeed higher, indicating that hydrogenation reactions occur preferentially. Also,

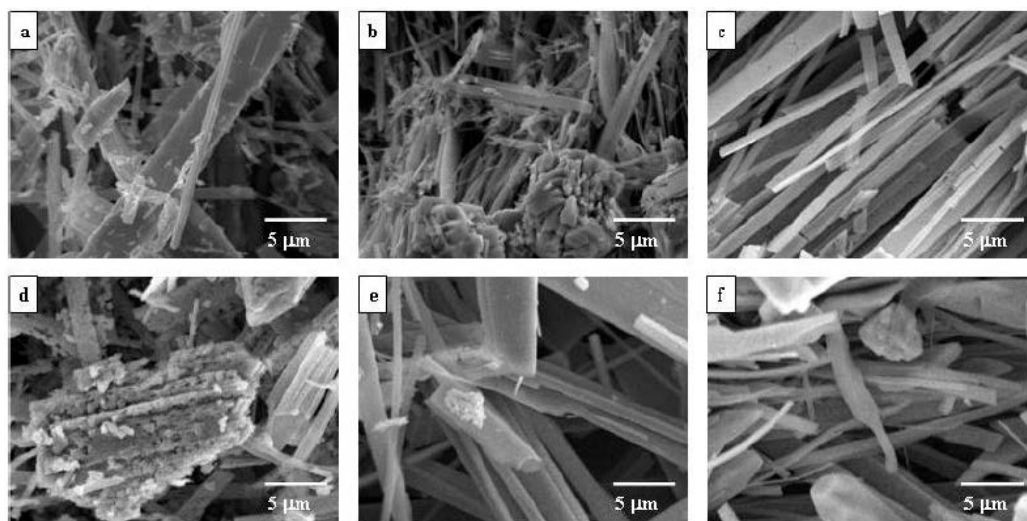


Figure 5. SEM micrographs of α -MoO₃, MS-400 and MS-500, before ((a)–(c)) and after ((d)–(f)) HDS of DBT.

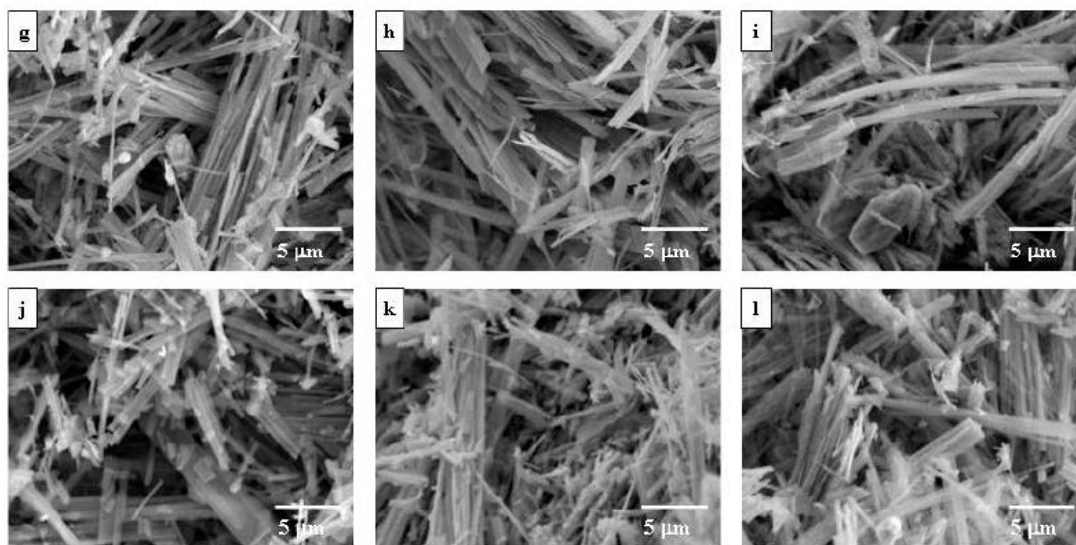


Figure 6. SEM micrographs for MS-600, MS-700, MS-800 before ((g)–(i)) and after ((j)–(l)) HDS of DBT.

Camacho et al [22] reported a HYD/DDS ratio of 1.8 using nanowires of MoS₂ in the HDS of DBT, under similar experimental conditions to those used here. In addition, since our experimental conditions are close to those used in industry, we believe that the difference in HYD/DDS ratio is probably due to a difference in the structure of the MoS₂. The Rim-edge model proposed by Daage and Chianelli [23] uses geometrical considerations and provides a direct relationship between the stacking height of layers and selectivity changes for HDS of DBT. ‘Rim’ sites located at the exterior of the stacked layers are active for hydrogenation and hydrogenolysis (C–S bond breaking) and ‘edge’ sites located on internal stacked layers are active only for hydrogenolysis. As was observed in the XRD patterns (figure 4(a)), the intensity of the (002) signal representative of the c direction layer stacking increased when the sulfidation temperature increased too. Therefore, according to the Rim-edge model, the MS-400, MS-500 and MS-600 catalysts show a higher preference for the HYD pathway compared to MS-700 and MS-800 catalysts, where the

stacking along 'c' direction is larger. The reaction rate coefficients (k) were calculated by assuming that HDS of DBT occurs following a pseudozero-order reaction rate expression. The k values presented in table 3 are of the same order of magnitude as those reported previously for MoS₂ catalysts: higher than the k value (1.7) found for ex situ single layers MoS₂ [24]; lower than that reported for in situ catalyst (6) [25], which shows an improvement in catalytic activity (attributed to its larger specific surface area); slightly lower than those for MoS₂ nanowires (3.7) [22]. All the k values mentioned are 10⁷ mol s⁻¹ g cat⁻¹. However, care must be taken in comparing the activities of these catalysts, since their specific surface areas are indeed different.

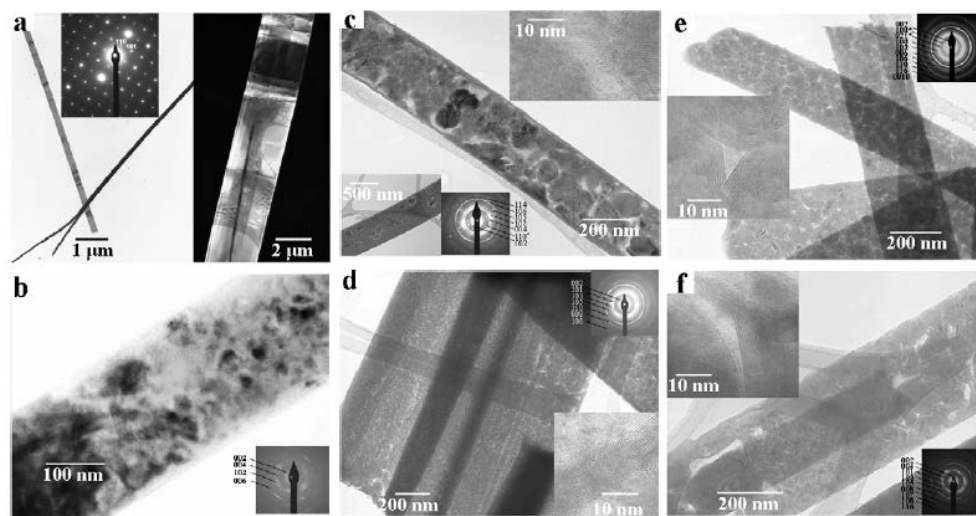


Figure 7. TEM micrographs of α -MoO₃ (a), MS-400 (b), MS-500 (c), MS-600 (d), MS-700 (e) and MS-800 (f) before HDS.

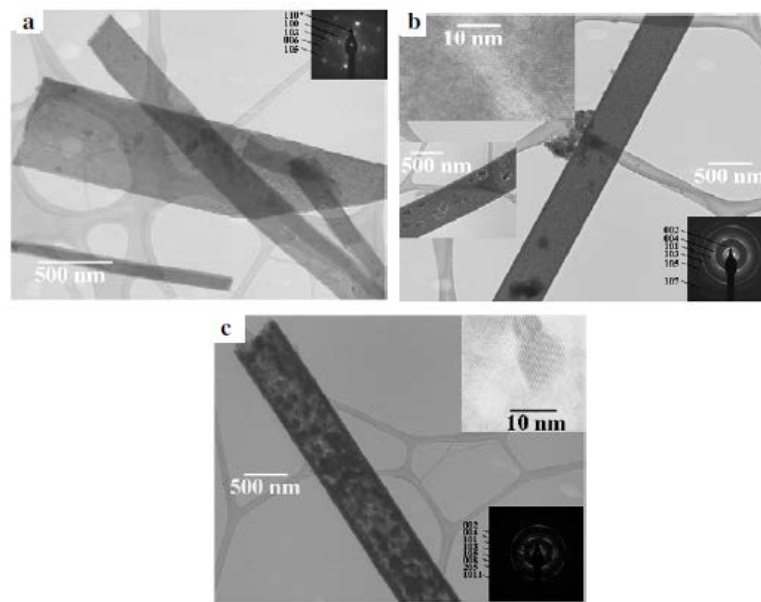


Figure 8. TEM micrographs of MS-400 (a), MS-500 (b) and MS-800 (c) after HDS.

The S/Mo ratios obtained by EDS for MS-800 and M-700 are similar to those reported for ex situ catalysts synthesized from tetra alkylammonium thiometallate precursors [23]. The MS-500 sample with an initial S/Mo ratio close to one presented the best catalytic activity in the HDS of DBT. This suggests that a partially sulfided catalyst (figure 4(a)) performs better for the HDS of DBT. According to the EDS and XRD results, it can be said that MS-500 is a partially sulfided material, with a theoretical formula $\text{MoS}_{2-x}\text{O}_x$ ($\alpha\text{-MoO}_3$, MoO_2 and MoS_2), with a value of x close to one. This partial sulfidation is perhaps responsible for the highest catalytic activity observed in our study, and the reason for having higher catalytic activities than those observed for ex situ MoS_2 catalyst [24].

4. Conclusions

The structure of the initial rods remains after sulfidation, however the formation of some holes in the final sulfide was observed. Even though our materials

exhibit low specific surface areas, they showed, in general, good catalytic activities in the HDS of DBT, comparable to other MoS₂ structures reported previously [22]. MS-500, a partially sulfided catalyst, showed the highest catalytic activity in this reaction. Finally, all samples exhibited higher HYD/DDS ratios, favouring preferentially the HYD reaction pathway, conversely to the low HYD/DDS ratios observed in industrial catalysts. This may be explained by considering the difference in the structure of the MoS₂

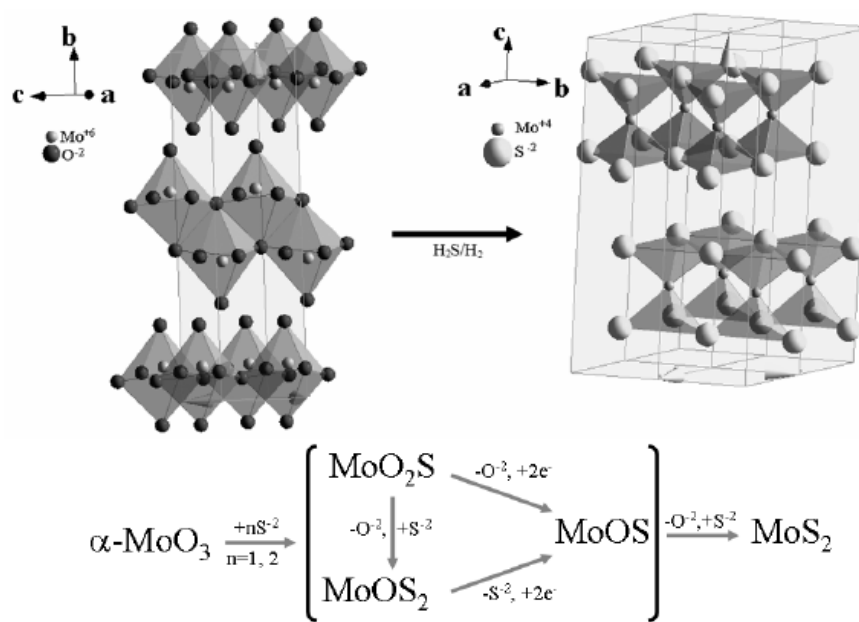


Figure 9. Transformation scheme for $\alpha\text{-MoO}_3$ into

MoS₂. Table 4. SAED indexing table.

MoS ₂		α -MoO ₃		MS400	MS500	MS600	MS700	MS800	MS400r	MS500r	MS800r		
JCPDF	<i>hkl</i>	JCPDF	<i>hkl</i>	(Å)	(Å)	(Å)	(Å)	(Å)	(Å)	(Å)	(Å)		
37-1492		75-0915											
6.16	002	3.77	110	6.13	6.14	3.69	6.15	6.15	3.86	6.14	3.60	6.17	6.16
3.07	004	3.24	021	2.91	2.92				3.26	3.04		3.06	3.08
2.74	100						2.76			2.75			
2.67	101	2.63	111				2.65		2.63			2.61	2.70
2.50	102	2.52	041	2.46	2.43								
2.28	103	2.27	150				2.23	2.25	2.26	2.26			2.27
2.05	006	2.00	160	1.99				1.91		2.12		2.20	
1.83	105	1.83	002		1.83	1.81			1.82	1.79		1.77	1.83
1.64	106	1.68	221	1.67	1.68			1.67					
1.58	110	1.60	250					1.60		1.62			
1.54	008	1.55	241				1.53		1.56				1.57
1.48	107	1.50	260		1.46				1.50	1.50	1.50	1.50	1.48
1.34	108	1.30	280	1.40			1.30		1.34				
1.25	116	1.26	082										
1.23	0010	1.22	340										
1.20	205	1.18	350					1.26	1.27				
1.10	118	1.11	272	1.11				1.22	1.18				1.25
1.04	1011												1.02
0.97	1110							1.05					
								0.96	0.99				

Acknowledgments

The authors thank Dr Mario Miki-Yoshida for fruitful discussions. We would like to thank C Ornelas, E Torres, D Lardizabal, Luis Licón, and W Antunez for their valuable technical assistance and the partial financial support of Conacyt, Project No. 40118-Y.

References

- [1] Iijima S 1991 Nature 354 56
- [2] Tenne R, Margulis L, Genut M and Hodes G 1992 Nature 360 443
- [3] Kis A, Mihailovic D, Remskar M, Mrzel A, Jesih A, Piwonski I, Kulik A J, Benoit W and Forró L 2003 Adv. Mater. 15 733
- [4] Rao C N R and Nath M 2003 Dalton Trans. 1 1
- [5] Remskar M, Skraba Z, Ballif C, Sanjines R and Levy F 1998 Surf. Sci. Rev. Lett. 5 423
- [6] Zelenski C M and Dorhout P K 1998 J. Am. Chem. Soc. 120 734

- [7] Nath M, Govindarai A and Rao C N R 2001 Adv. Mater. 13 283
- [8] Wen K H, Bao H C, Yan Q Z, Wei Q H, Terrones H, Terrones M, Grober N, Cheetham A K, Krato H W and Walton DRM 2000 J. Am. Chem. Soc. 122 10155
- [9] Li Q, Newberg J T, Walter E C, Hemminger J C and Penner R M 2004 Nano Lett. 4 277
- [10] Santiago P, Ascencio J A, Mendoza D, Perez-Alvarez M, Espinoza A and Reza-Sangerman C 2004 Appl. Phys. A 78 513
- [11] Zheng X, Zhu L, Yan A, Bai C and Xie Y 2004 Ultrason. Sonochem. 11 83
- [12] Tian Y, He Y and Zhu Y 2004 Mater. Chem. Phys. 87 87
- [13] Zepeda T A, Halachev T, Pawelec B, Nava R, Klimova T, Fuentes G A and Fierro J L G 2006 Cat. Commun. 7 33
- [14] Wen Lou X and Zeng H C 2002 Chem. Mater. 14 4781
- [15] Leisegang T, Levin A A, Walter J and Meyer D C 2004 Cryst. Res. Technol. 40 95.